# PROPERTIES OF THE 960-MeV BOSON*

P. M. Dauber, W. E. Slater, L. T. Smith, D. H. Stork, and H. K. Ticho
Department of Physics, University of California, Los Angeles, California
(Received 19 August 1964)

Recently two groups[1,2] reported the existence of a narrow nonstrange boson resonance with a mass near 960 MeV. This resonance (labeled temporarily) $X^0$ was produced in the reaction

$$K^- + p \rightarrow \Lambda + X^0, \tag{1}$$

and decayed mainly through

$$X^0 \rightarrow \pi + \pi + \eta. \tag{2}$$

We wish to report the observation of $X^0$ in the same reaction using the Lawrence Radiation Laboratory 72-in. hydrogen bubble chamber, and incident kaons with momenta of 1.80 and 1.95 GeV/$c$. Figure 1 shows histograms of the invariant mass squared of the particles produced in addition to the $\Lambda$ in the reactions

$$K^- + p \rightarrow \Lambda + \text{neutrals} \tag{3}$$

$$\rightarrow \Lambda + \pi^+ + \pi^+ \tag{4}$$

$$\rightarrow \Lambda + \pi^+ + \pi^- + \pi^0 \tag{5}$$

$$\rightarrow \Lambda + \pi^+ + \pi^- + \text{neutrals} \tag{6}$$

$$\rightarrow \Lambda + 2\pi^+ + 2\pi^- \tag{7}$$

$$\rightarrow \Lambda + 2\pi^+ + 2\pi^- + \text{neutral(s)}. \tag{8}$$

The effective mass of fitted events is used for Reactions (4), (5), and (7), and missing mass above $\Lambda$ ($MM_\Lambda$) for the others. For events of class (6) the additional requirement $MM_{\Lambda\pi^+\pi^-}$

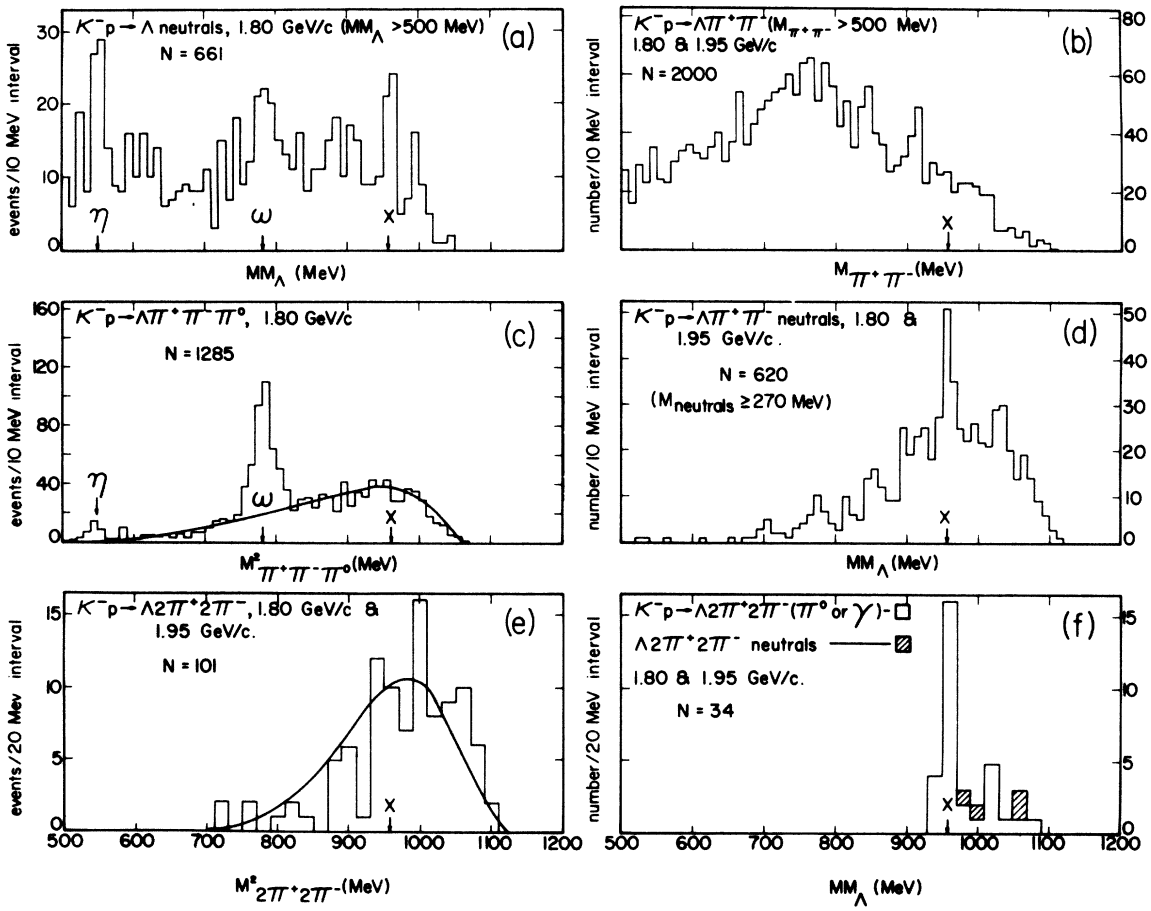


FIG. 1. Effective-mass plots and missing mass above $\Lambda$ plots for various reactions of the $K^- + p \rightarrow \Lambda$ + boson(s) type.

> 270 MeV was imposed. The peak due to the $X^0$ shows up most clearly in Reaction (8); the events which fit the reactions $2\pi^+2\pi^-\pi^0$ and $2\pi^+2\pi^-\gamma$ are indicated in Fig. 1(f). The $X^0$ peak is also distinguished in Reactions (3) and (6), but not in Reactions (4), (5), and (7). For Reactions (5) and (7) the invariant phase space normalized to the number of events is also shown.

Figure 2(a) shows a scatter plot of $MM_\Lambda$ vs $MM_{\Lambda\pi^+\pi^-}$ for those examples of (6) which satisfy $890 < MM_\Lambda < 1030$ MeV, $460 < MM_{\Lambda 2\pi} < 640$ MeV. It is clear that a large fraction of the excess above background due to the $X^0$ consists of events where the emitted neutrals have the $\eta$ mass; i.e., that $X^0$ undergoes $\pi^+\pi^-\eta_0$ decay. In view of this all examples of (6) were fitted using the one-constraint hypothesis $\Lambda\pi^+\pi^-\eta_0$. Figure 2(b) shows an ideogram of effective mass of the $\pi^+\pi^-\eta_0$ system for 85 events of type (6) which fit the $\Lambda\pi^+\pi^-\eta_0$ hypothesis with $\chi^2 < 8.0$. Also shown in Fig. 2(b) is the resolution function based on the a priori measurement errors of the events in the vicinity of the $X^0$ peak. The resolution curve has been normalized to the events above background and has been widened by a factor of $(2)^{1/2}$ such that it and the ideogram of the resonance should coincide for a resonance with $\Gamma = 0$. Within errors, the data are evidently consistent with $\Gamma_{X^0} = 0$. Using a Monte Carlo procedure in which the resonant peak was artificially widened in accordance with Breit-Wigner curves of known $\Gamma$, we find $\Gamma_{X^0} < 4$ MeV with a 90% confidence limit. The peak lies at 957 MeV.

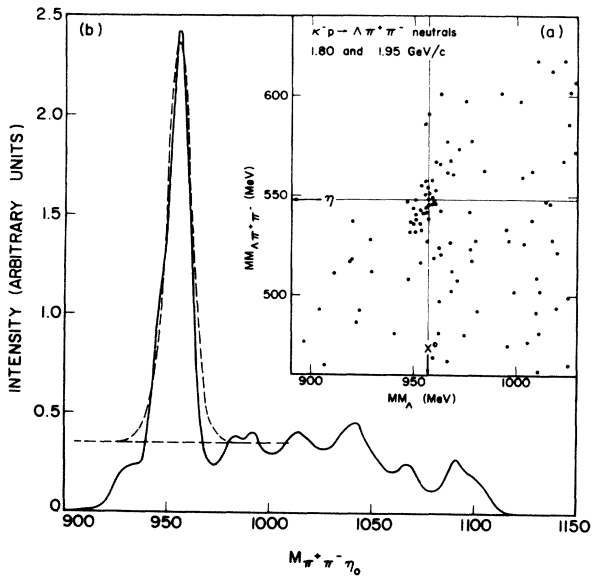


FIG. 2. (a) Scatter plot based on raw measurements of the missing mass above $\Lambda$, $MM_\Lambda$, versus missing mass above $\Lambda\pi^+\pi^-$, $M_{\Lambda\pi^+\pi^-}$, for the reaction $K^- + p \to \Lambda + \pi^+ + \pi^- +$ neutrals. No fitting of the events was carried out. (b) Ideogram of the effective mass of the $\pi^+\pi^-\eta_0$ system for the same events fitted to the $K^- + p \to \Lambda + \pi^+ + \pi^- + \eta_0$ hypothesis.

In view of the sharpness of the resonance and the dominance of the $2\pi\eta$ decay channel, all the examples of Reactions (6) and (8) have been fitted to the hypothesis "$X$" in which the event is interpreted as a two-step sequence $K^- + p \to \Lambda + X^0$, $X^0 \to \pi^+ + \pi^- + \eta$, assuming $M_{X^0} = 957$ MeV, $M_\eta = 548$ MeV. In the examples of (6), $\eta_0$ decay was postulated; 38 events fit both production and decay with $\chi^2 < 8.0$. For the examples of (8) there exists an eightfold ambiguity: The $\eta$ may be assumed to decay either via $\pi^+\pi^-\pi^0$ or $\pi^+\pi^-\gamma$ and, in addition, there are two choices each for the charged pions. Of the 20 events of Reaction (8) which fit hypothesis "$X$," 14 fit unambiguously (11 as $\pi^+\pi^-\pi^0$ and three as $\pi^+\pi^-\gamma$). In the six ambiguous cases there exist two combinations which fit $\eta_C$ decay. These were adjudicated on the basis of the lower $\chi^2$ fit. The fits using $M_{X^0} = 957$ MeV are used in the following analysis.

The production process insures that $X^0$ has isospin $T = 0$ or 1. The isoparity of the decay products of $X^0$ is $G = +1$. However, since $\Gamma_{X^0} = 0$ within experimental errors, the possibility that the $X^0 \to 2\pi + \eta$ decay is electromagnetic with $|\Delta I| = 1$, $\Delta G =$ yes cannot be immediately discarded. If the $X^0 \to 2\pi + \eta$ decay is electromagnetic, then $X^0$ has $G = -1$. Such an object can decay strongly into $3\pi$ for all spin-parity $J^P$ assignments (apart from $0^+$ which is forbidden to $2\pi\eta$ as well). The phase space for $3\pi$ decay is larger than the $2\pi\eta$ phase space by a factor of ~17. In addition, in contrast to the $2\pi\eta$ decay, $3\pi$ decay, if present, would be relativistic and angular-momentum barriers would be expected to play a less significant role. Finally, the approximate selection rule[3] based on the conjectured quantum number $A$ would effect the $3\pi$ and the $2\pi\eta$ decay equally since both $\pi$ and $\eta$ are supposed to have $A = -1$. Experimentally, using the data of Fig. 1, one may set the branching ratio $(X^0 \to 3\pi)/(X^0 \to 2\pi + \eta) \simeq 0.0 \pm 0.2$. Including the $\alpha^2$ factor required for electromagnetic $2\pi\eta$ decay, this ratio is smaller than expected by a factor of ~$10^6$. It seems very likely therefore that $X^0 \to 2\pi + \eta$ represents a strong decay, and we shall assume that $X^0$ has $G = +1$.

The Dalitz-Fabri plot of the $X^0$ is shown in Fig. 3(a). All events have been fitted using hy-

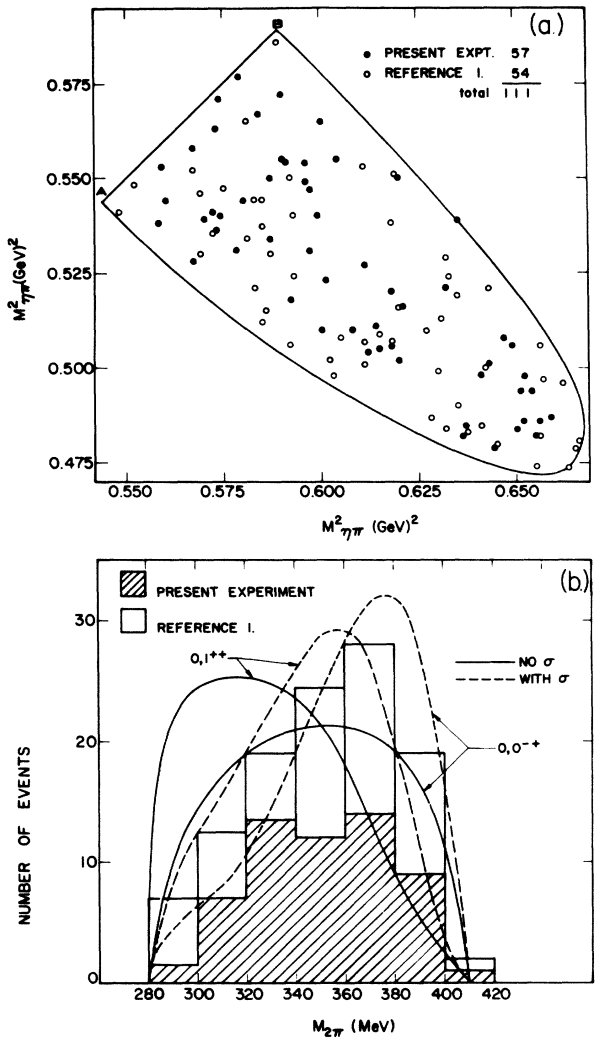


pothesis "$X$"; hence, the kinematic boundary is sharp.[4] In order to increase the statistical precision, the data of reference 1, fitted in the same way,[5] have been added. The number of background events in the plot is estimated to be <9%. The third column of Table I gives the density $D$ of points within the Dalitz "ellipse" for $T=0$ and $T=1$ and for various $J^P$ assignments with $J<3$. The quantities $p$, $q$, and $\theta$ are, respectively, the $\eta$ momentum in the $X^0$ rest frame, the pion momentum, and the angle between these momenta, both in the di-pion rest frame. Only the first terms of the expansions of the densities in terms of $p^2$ and $q^2$ are retained in Table I. In view of the low $Q$ value of 129 MeV of the decay this should be a good approximation provided there are no strong final-state interactions. The amplitudes $a$ and $b$ in the $T(J^{PG})=0(2^{-+})$ case correspond to the $(l,L)=(0,2)$ and $(2,0)$ choices, respectively; $l$ is the interval angular momentum of the di-pion and $L$ the over-all orbital angular momentum.

The data have been fitted to the densities $D$ in Table I by means of a maximum-likelihood

FIG. 3. (a) Dalitz-Fabri plot for the decays $X^0\to\pi^+ +\pi^- +\eta_0$ and $X^0\to\pi^+ +\pi^- +\eta_c$ for events fitted to hypothesis "$X$": $K^- +p\to\Lambda +X^0$, $X^0\to 2\pi+\eta$. Charge symmetry permits folding about the AB line. (b) Histogram of the effective mass of the di-pion in $X^0\to 2\pi +\eta$. The smooth curves represent phase space $\Phi$ appropriate to a $0^-$ particle, $p^2\Phi$ for a $1^+$ particle. The dashed curves include the effect of the $\sigma$.

Table I. Dalitz-plot densities for $T=0$, 1, and various $J^P$ assignments, and results of maximum-likelihood fitting procedure.

| $T$ | $J^P$ | $D_{J,P,T}$ | $\Delta/\nu$ This expt. | $\Delta/\nu$ This expt. plus data of Kalbfleisch et al.[b] | $\Delta/\nu$ with $\sigma$[a] This expt. | $\Delta/\nu$ with $\sigma$[a] This expt. plus data of Kalbfleisch et al.[b] |
|---|---|---|---|---|---|---|
| 1 | $0^-$ | $p^2q^2\cos^2\theta$ | −13.7 | −16.7 | | |
| | $1^+$ | $q^2$ | − 3.0 | − 4.3 | | |
| | $1^-$ | $p^2q^2\sin^2\theta$ | − 4.0 | −10.1 | | |
| | $2^+$ | $p^4q^2\sin^2\theta$ | − 6.5 | −14.5 | | |
| | $2^-$ | $p^2q^2(1+\frac{1}{3}\cos^2\theta)$ | − 1.2 | − 3.2 | | |
| 0 | $0^-$ | 1 | + 1.6 | + 0.9 | −1.3 | −2.3 |
| | $1^+$ | $p^2$ | − 4.3 | − 8.4 | −0.5 | −2.7 |
| | $1^-$ | $p^4q^4\cos^2\theta\sin^2\theta$ | −11.5 | −16.7 | | |
| | $2^+$ | $p^2q^4\sin^2\theta$ | − 6.2 | −12.4 | | |
| | $2^-$ | $\{\lvert a\rvert^2p^4+\lvert b\rvert^2q^4\}$ $+3\,\mathrm{Re}ab^*p^2q^2(\cos^2\theta-\frac{1}{3})$ | | [c] | | |

[a]Using $D'=D[(M_{2\pi}{}^2-M_\sigma{}^2)^2+(M_\sigma\Gamma_\sigma)^2]^{-1}$ with $M_\sigma=380$ MeV, $\Gamma_\sigma=80$ MeV.
[b]See reference 1.
[c]Because of the availability of the fitting parameter $b/a$, the procedure is different in this case. The data fit well for $b/a\sim 3$.

procedure. Let

$$f_{J,P,T} = C_{J,P,T}\mathcal{J}D_{J,P,T}$$

where $C$ normalizes $f$ such that $\int\int f dq^2 d\cos\theta = 1$ and $\mathcal{J} = 4M_X\phi q/(M_\pi{}^2+q^2)^{1/2}$ is the Jacobian such that $dM_{\eta\pi}{}^2 dM_{\eta\pi}{}^2 = \mathcal{J} dq^2 d\cos\theta$. Then

$$\Delta_{J,P,T} = \frac{1}{N}\sum_i^N [\ln f_{J,P,T}(q_i{}^2, \cos\theta_i) - \langle \ln f_{J,P,T}\rangle], \quad (9)$$

$$\nu_{J,P,T}{}^2 = (1/N)[\langle (\ln f_{J,P,T})^2\rangle - \langle \ln f_{J,P,T}\rangle^2], \quad (10)$$

where $\langle g\rangle = \int\int f g dq^2 d\cos\theta$. The sum ranges over the $N$ experimental $(q_i{}^2, \cos\theta_i)$ pairs. The quantity $\Delta/\nu$ given in Table I is the mean deviation of the experimental likelihood from the theoretical value for each $J^P$ and $T$ value measured in terms of the appropriate variance.

An examination of Table I shows that the data fit well for $0(0^{-+})$. They can also be made to fit the $0(2^{-+})$ hypothesis—but in this case there is an adjustable parameter $b/a$ available. The data fit for $b/a \sim 3$. The best $T=1$ fit is obtained for $1(2^{-+})$. To check whether the quantity $\nu$ can be treated as a standard deviation in the usual sense, 1731 "experiments" of 111 counts each were generated by Monte Carlo techniques according to the $1(2^{-+})$ density. Of the 1731 "experiments" only 2 exceeded $\Delta/\nu = 3.2$. The $1(2^{-+})$ assignment is therefore very improbable.

Figure 3(b) shows the projection of the decay data on the $M_{\pi^+\pi^-}$ axis. Also shown are curves for phase space, $\Phi(M_{2\pi})$, and $p^2\Phi(M_{2\pi})$, appropriate, respectively, to $J^P = 0^-$ and $1^+$ in the absence of $\pi$-$\pi$ interaction. To first approximation in both these cases the final state $\pi$-$\pi$ system is emitted in an $s$ state. Present evidence[6-8] suggests the possibility of a $T=J=0$ $\pi$-$\pi$ resonance[9] $\sigma$ with $M_\sigma \simeq 380$ MeV, $\Gamma_\sigma \simeq 80$ MeV. In the remaining two curves of Fig. 3(b) the effect of this possible resonance is included by means of a resonance denominator $[(M_{2\pi}{}^2 - M_\sigma{}^2)^2 + (M_\sigma\Gamma_\sigma)^2]^{-1}$. This resonance denominator was also used as a factor in the Dalitz plot densities used in maximum likelihood fits. The results for this case are given in the last two columns of Table I. It seems likely that within the present uncertainties in the $\sigma$ parameters suitable values may be chosen to effect a good fit for $0(0^{-+})$, $0(1^{++})$, or $0(2^{-+})$.

The production angular distributions for 1.80 and 1.95 GeV/$c$ are shown in Fig. 4(a). As was already noted[1,2] the $X^0$'s generated in (1) are sharply peaked forward which suggests the dominance of a peripheral production mechanism. An object with $J^P = 0^-$, $1^+$, or $2^-$ cannot result from $K$ exchange. It seems likely, therefore, that the production process should be described by $K^*$ exchange. Figure 4(b) shows a scatter plot of the direction of the normal to the $X^0$ decay plane. The angles $\beta$ and $\varphi$ are the polar and azimuthal coordinates in a reference frame in which the $X^0$ is at rest and the $z$ and $y$ axes are the incident $K^-$ direction and the normal to the production plane, respectively.

For a $1^+$ particle the distribution function of

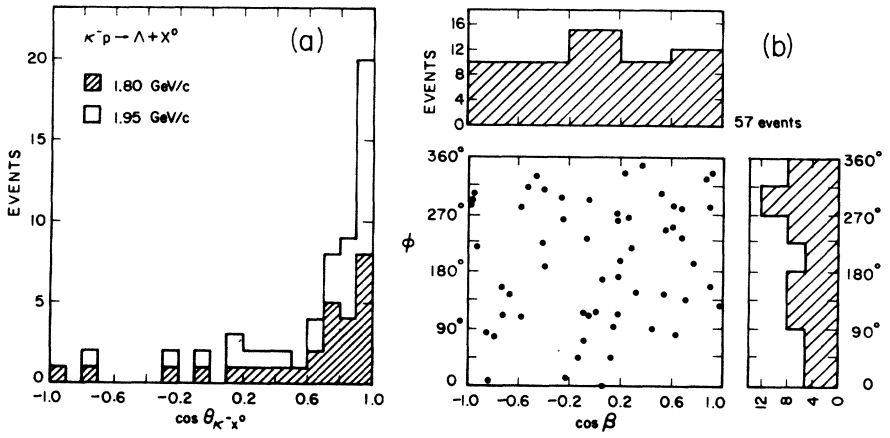


FIG. 4. (a) $X^0$-production angular distribution. (b) Scatter plot (and its projections) of the direction of the normal to the decay plane. For definition of coordinate system see text.

the normal has the form[10]

$$w(\cos\beta,\varphi)=N\{(1-2\rho_{1,1})\cos^2\beta+\rho_{1,1}\sin^2\beta-\rho_{1,-1}\sin^2\beta\cos2\varphi-\sqrt{2}\,\mathrm{Re}(\rho_{1,0})\sin2\beta\cos\varphi)\},\quad(11)$$

where $\rho_{i,j}$ are the elements of the density matrix of the decaying particle and $N$ is a normalization constant. The assumption of $K^*$ exchange does not produce a simplification of the relation. A $2^-$ particle formed in a $\bar{K}$-$K^*$ collision cannot have $z$ components of angular momentum $m=\pm2$; hence, the density matrix elements referring to $m=\pm2$ vanish when $K^*$ exchange is invoked. After integration over $\varphi$, the distribution function[11] becomes

$$W(\cos\beta)=N\{7+5(1-2|a_0|^2)(1+\rho_{00})P_2(\cos\beta)+(5|a_0|^2+1)(5\rho_{00}-2)P_4(\cos\beta)\},\quad(12)$$

where $a_0$ is the probability amplitude that the component of angular momentum along the decay normal vanishes; $0<|a_0|^2<1$.

The experimental distribution in $\cos\beta,\varphi$ appears flat within statistics. Parity conservation permits folding of the scatter plot both about $\cos\beta=0$ and about $\varphi=180°$. A flat distribution is consistent with the $0^-$ assignment to $X^0$. According to Eqs. (11) and (12) it can also be made consistent with the $1^+$ and $2^-$ assignments for special choices of the density-matrix elements and of the decay parameter $|a_0|^2$ in the $2^-$ case.

At 1.80 GeV/$c$ 28 $X^0\to\pi^+\pi^-\eta$ decays were observed. If $T=0$, then $14\pm3$ $X^0\to2\pi^0\eta$ decays are expected, or $10\pm3$ via $X^0\to2\pi^0\eta_0$. Using Fig. 1(a), $21\pm5$ events are estimated to be in the all-neutral $X_0$ peak. Because of the low statistics it is not clear whether the excess of $11\pm6$ is real. However, it is perhaps worth noting that $4\pi^0$ decay would be more strongly inhibited by angular-momentum barriers than $2\pi^+2\pi^-$ decay for $T=0$, $J^P=0^-$, $1^+$, or $2^-$. From Fig. 1(e) the ratio $(X^0\to2\pi^+2\pi^-)/(X^0\to\pi^+\pi^-\eta)=0.00\pm0.04$. Furthermore, $\pi^0\gamma$ and $2\pi^0\gamma$ decays are entirely forbidden for these quantum number assignments; thus, second-order decays such as $2\gamma$ or $\pi^02\gamma$ would have to be invoked.

Finally, a search was made for the $X^0\to\pi^+\pi^-\gamma$ decay. With this in view an attempt was made to fit all events of the $\Lambda$ two-prong topology which did not fit $\Lambda\pi^+\pi^-$ to the hypotheses $\Lambda\pi^+\pi^-\gamma$ and $\Lambda\pi^+\pi^-\pi^0$. Figure 4(a) shows that 64% of $\Lambda X^0$ events have $\cos\theta_{K^-X}^{\text{c.m.}}\geq0.70$. Therefore, to reduce backgrounds only events with $\cos\theta_{K^-\Lambda}^{\text{c.m.}}\leq-0.70$ were used in the search for the $\pi^+\pi^-\gamma$ decay. Events with $\chi^2\geq8$ for both hypotheses were rejected (as presumably due to the emission of more than one neutral particle). Region A in Fig. 5(a) was defined as unambiguous for $\Lambda\pi^+\pi^-\gamma$ events, while in region B $\Lambda\pi^+\pi^-\gamma$ and $\Lambda\pi^+\pi^-\pi^0$ events could not be distinguished on the basis of $\chi^2$'s. Figures 5(b) and 5(c) show the effective $\pi^+\pi^-\gamma$ mass histograms for these two classes of events. The shaded events in both histograms are those which also satisfied the $\Sigma^0\pi^+\pi^-$ hypothesis (2C) with a $\chi^2\leq16$. Clearly, most unambiguous $\Lambda\pi^+\pi^-\gamma$ events are in fact $\Sigma^0\pi^+\pi^-$ events. If all the excess events above background in both regions A and B are interpreted as due to $X^0\to\pi^+\pi^-\gamma$ decay, then the ratio of decay rates $(X^0\to\pi^+\pi^-\gamma)/(X^0\to2\pi\eta)=0.25\pm0.14$.

The 1.80- and 1.95-GeV/$c$ data therefore support the existence of a nonstrange boson with mass 957 MeV. Its width is $\Gamma_{X^0}<4$ MeV with 90% confidence limit. The absence of intense $3\pi$ decay strongly suggests that the decay is strong; hence, $G=+1$. The Dalitz plot is consistent with $T=0$, the $J^P=0^-$ and $2^-$ assignments, and also $1^+$ if

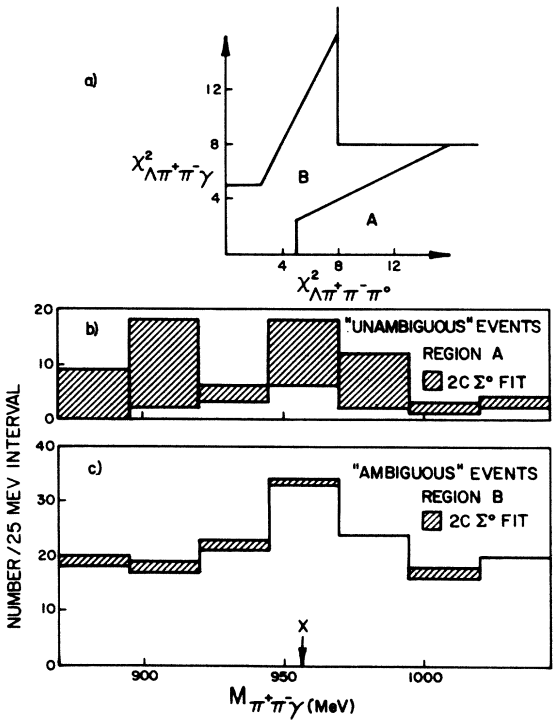


FIG. 5. (a) Definition of unambiguous and ambiguous regions for $\Lambda\pi^+\pi^-\gamma$ and $\Lambda\pi^+\pi^-\pi^0$ fits. (b) $\pi^+\pi^-\gamma$ histogram for unambiguous events. (c) $\pi^+\pi^-\gamma$ histogram for ambiguous events.

the $\sigma$ resonance is invoked. The distribution in the decay normal is consistent with $0^-$. It is also consistent with $1^+$ and $2^-$, but only under rather special circumstances. These findings agree with the work of the other groups[1,2] wherever the data can be compared. For $T=0$, and correcting for neutral $\Lambda$ decays, the $X^0$ production cross section averaged over the 1.80- to 1.95-GeV/$c$ momentum range is $54 \pm 8$ $\mu$b.

We wish to thank the members of the Lawrence Radiation Laboratory 72-in. hydrogen bubble chamber group, and particularly Professor L. W. Alvarez, for their continuing friendly cooperation. Our gratitude is due Professor Charles Zemach, Dr. R. C. Arnold, and Dr. S. Fenster for many stimulating discussions. Finally, we acknowledge our indebtedness to our patient and conscientious scanning staff.

*Work supported in part by the U. S. Atomic Energy Commission.

[1]G. R. Kalbfleisch et al., Phys. Rev. Letters 12, 527 (1964).

[2]M. Goldberg et al., Phys. Rev. Letters 12, 546 (1964).

[3]J. B. Bronzan and F. E. Low, Phys. Rev. Letters 12, 522 (1964).

[4]If the $X^0$ mass is permitted to vary within $M_{X^0} \pm \Gamma_{X^0}/2$ with $M_{X^0}=957$ MeV and $\Gamma_{X^0}=4$ MeV, the area within the Dalitz plot changes by 6%.

[5]We wish to thank Dr. G. R. Kalbfleisch for making the data available to us.

[6]L. M. Brown and P. Singer, Phys. Rev. 133, B812 (1964). For considerations of the effect of the $\sigma$ on $X^0$ decay see L. M. Brown and H. Faier, Phys. Rev. Letters 13, 73 (1964).

[7]F. S. Crawford, R. A. Grossman, L. J. Lloyd, L. R. Price, and E. C. Fowler, Phys. Rev. Letters 11, 564 (1963).

[8]R. Del Fabbro et al., Phys. Rev. Letters 12, 674 (1964).

[9]See, however, G. E. Kalmus, A. Kernan, R. T. Pu, W. Powell, and R. Dowd, Phys. Rev. Letters 13, 99 (1964).

[10]This is the same distribution as that given for the decay of a $1^-$ particle into two spinless bosons by K. Gottfried and J. D. Jackson, Phys. Letters 8, 144 (1964).

[11]R. C. Arnold and S. Fenster, private communication.

## $s$-WAVE $\pi\pi$ INTERACTION AND $K_1^0K_2^0$ MASS DIFFERENCE*

Sharashchandra H. Patil†
University of California San Diego, La Jolla, California
(Received 31 August 1964)

In a recent paper[1] the $s$-wave $\pi\pi$ interaction was analyzed with reference to various pieces of experimental data, in particular, the $K_1^0K_2^0$ mass difference which was assumed to be due to the $2\pi$ decay mode of $K_1^0$. Various models[1-3] have been discussed in connection with this mechanism of the mass difference. Recently, however, there has been an alternative proposition[4,5] that the mass difference comes from the pole due to $\pi$ and $\eta$ intermediate states in the self-energy graphs of $K_2^0$. In one version[4] of this scheme the $K_2^0$ is heavier than $K_1^0$, while in the other version[5] the $K_1^0$ is heavier than $K_2^0$ by almost an equal amount. In both the versions the magnitude of the mass difference is approximately proportional to $g_{K\pi}^2$ where $g_{K\pi}$ is the $K\pi$ weak coupling. If one calculates $g_{K\pi}^2$ from the $\mu^+\nu$ decays of $K^+$ and $\pi^+$ and assuming the $\Delta I=\frac{1}{2}$ rule, the $g_{K\pi}^2$ obtained is found to be too small[4] by a factor of about 30 to explain the $K_1^0K_2^0$ mass difference. On the other hand, arguments are presented in reference 4 to show that this coupling can be large.

In this paper we study the $3\pi$ decay mode of $K_2^0$ via a single-pion pole and hence try to get information about the $K\pi$ coupling directly without recourse to leptonic decay modes. We first assume that in the decay $K_2^0 \to \pi^0 \to \pi^+ + \pi^- + \pi^0$, the $\pi^+$ and $\pi^-$ are in the $I=0$ $s$-wave state, and given the partial width for this decay we discuss the $K\pi$ coupling for various models of $s$-wave $\pi\pi$ interaction. In all the models we discuss, the $g_{K\pi}^2$ coupling comes out to be of the same order as obtained from $\mu^+\nu$ decay modes of $K^+$ and $\pi^+$, and hence in disagreement with the $\pi,\eta$ pole mechanism for explaining the $K_1^0K_2^0$ mass difference. We also calculate the effect of $p$-wave $\pi\pi$ interaction in the form of the $\rho$ meson and find its effect to be negligible.

Consider the decay width for the reaction

$$K_2^0 \to \pi^+ + \pi^- + \pi^0 \qquad (1)$$

via the $\pi^0$ pole diagram of Fig. 1. This is the most important diagram contributing to the above reaction from the dispersion-relation point of